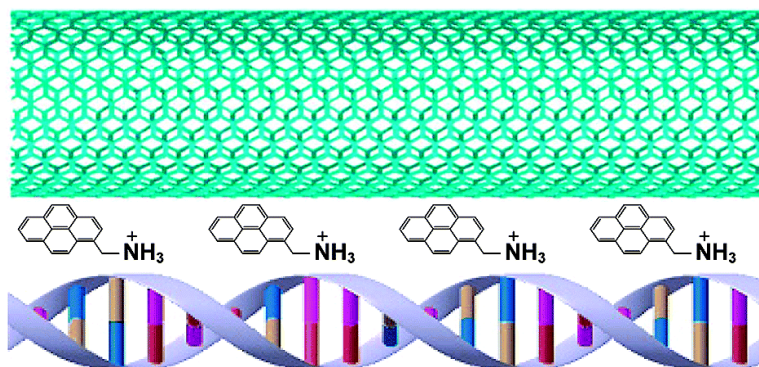


## DNA-Templated Nanotube Localization

Huijun Xin, and Adam T. Woolley

*J. Am. Chem. Soc.*, **2003**, 125 (29), 8710-8711 • DOI: 10.1021/ja035902p • Publication Date (Web): 25 June 2003

Downloaded from <http://pubs.acs.org> on March 29, 2009



### More About This Article

Additional resources and features associated with this article are available within the HTML version:

- Supporting Information
- Links to the 12 articles that cite this article, as of the time of this article download
- Access to high resolution figures
- Links to articles and content related to this article
- Copyright permission to reproduce figures and/or text from this article

[View the Full Text HTML](#)



## DNA-Templated Nanotube Localization

Huijun Xin and Adam T. Woolley\*

*Department of Chemistry and Biochemistry, Brigham Young University, Provo, Utah 84602-5700*

Received May 1, 2003; E-mail: atw@byu.edu

The construction and evaluation of materials and devices with nanometer dimensions has become an area of rapidly expanding research interest. Carbon nanotubes have emerged as important materials for nanofabrication, in both electronic devices<sup>1</sup> and sensors.<sup>2</sup> A key issue in the use of carbon nanotubes in nanofabrication is the need for their controlled placement at well-defined positions on surfaces. Previous efforts to control localization of nanotubes or nanorods have included the use of microfluidics,<sup>3</sup> an applied electric field,<sup>4</sup> or patterning using side edges of multilayer films.<sup>5</sup> An intriguing approach for assembly of nanoscale materials is the use of a biological template to direct the positioning of components on a surface. DNA is an attractive candidate template, since it possesses a small diameter (~2 nm), controllable length that can exceed 10  $\mu\text{m}$ , and the ability to use molecular recognition in forming specific base pairs. Indeed, recent work has demonstrated the application of DNA in construction of various types of metallic nanowires.<sup>6</sup> In this work, we report a novel method that enables selective localization of single-walled carbon nanotubes (SWNTs) on aligned DNA molecules on surfaces. This approach represents a simple route to manipulation and positioning of SWNTs on surfaces, and provides an important tool in bottom-up biotemplated nanofabrication.

Our approach for directed placement of SWNTs on surfaces involves aligning DNA on a substrate, treating the surface with a bifunctional bridging compound, and then exposing the substrate to a SWNT suspension. Double-stranded  $\lambda$ -DNA was linearly aligned on a Si surface that had been treated with 1 ppm aqueous poly-L-lysine, following a previously developed method.<sup>7</sup> Next, the Si with aligned DNA was submerged in a 6 mM solution of 1-pyrenemethylamine hydrochloride (PMA) (Aldrich, Milwaukee, WI) in *N,N*-dimethylformamide (DMF) (EM Science, Gibbstown, NJ) for 12 h in the dark. Finally, a 40- $\mu\text{L}$  droplet of a 0.1 mg/mL acid-purified SWNT (Carbon Solutions Inc., Riverside, CA) suspension in DMF<sup>8</sup> was pipetted onto the Si substrate and allowed to sit for 20 min. Between each step, the substrates were rinsed thoroughly with deionized water, or with both DMF and water, and dried under a stream of compressed air. In a control experiment, we directly exposed a Si substrate with aligned DNA to the SWNT suspension, without the PMA treatment step.

Figure 1 shows an atomic force microscopy (AFM) height image of  $\lambda$ -DNA aligned on a Si surface and treated with PMA; for comparison, the inset depicts a surface with aligned  $\lambda$ -DNA not exposed to PMA.<sup>9</sup> Round elevated features along the DNA are indicative of clusters of PMA that decorate the DNA; in addition, a small amount of nonspecific deposition of PMA clusters is observed on the Si surface.<sup>10</sup> The amine group in PMA is expected to interact electrostatically with the negatively charged phosphate backbone of DNA, while the aromatic pyrenyl group is known to interact strongly with the surfaces of SWNTs through  $\pi$ -stacking forces.<sup>11</sup> Thus, the localization of PMA primarily on the DNA should enable the specific assembly of SWNTs on surface DNA molecules.

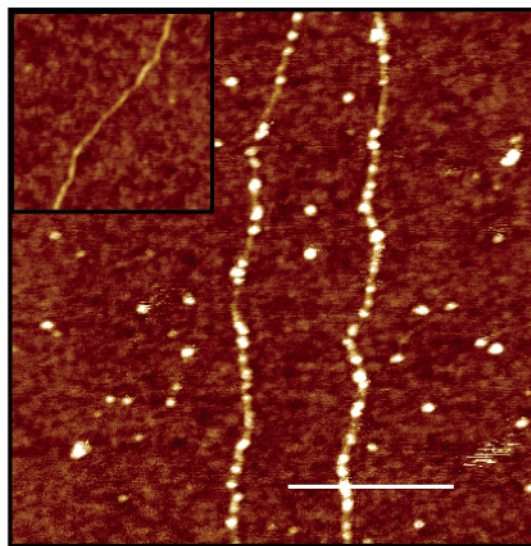


**Figure 1.** AFM height images of untreated (inset) and PMA-treated  $\lambda$ -DNA aligned on a Si surface. The height scale is 6 nm, and the white bar indicates 250 nm.

We used AFM to image three different Si substrates that had SWNTs deposited onto PMA-treated, aligned DNA. We obtained 60 images on these substrates, covering an area of  $\sim 600 \mu\text{m}^2$  on each surface. Representative AFM images from these surfaces are shown in Figure 2. All three images show aligned DNA and one or more SWNTs specifically localized on the nucleic acid template. Nanotube heights range from 1.3 to 9 nm, suggesting that a mixture of SWNT bundles and individual SWNTs has been deposited. From the 60 AFM images on all three substrates, we determined that 63% of SWNTs observed on the surface were anchored along DNA, while the DNA itself covered only  $\sim 1\%$  of the surface area. The lack of perfect selectivity in SWNT placement can be explained in part by the presence of some nonspecifically deposited PMA on the surfaces. Importantly, on a control substrate where the DNA was not treated with PMA, only  $\sim 10\%$  of the SWNTs were aligned on DNA; these results suggest that PMA plays a key role in the selectivity of SWNT deposition onto surface DNA.

The AFM data in Figure 2 indicate incomplete coverage of the surface DNA with SWNTs. In 12 typical images, we measured the total length of all surface DNA, as well as the total length of specifically deposited SWNTs. From these measurements we determined that, on average,  $\sim 5\%$  of the total DNA length was covered with specifically aligned SWNTs. We attribute the partial coverage to three factors. First, stable SWNT suspensions could be made only at concentrations  $\leq 0.1 \text{ mg/mL}$ , which limited the total number of SWNTs available for localization on surface DNA. Suspensions with higher SWNT concentrations tended to aggregate and precipitate. Second, in the suspension, only SWNTs that are nearly parallel with aligned DNA have a strong interaction with the PMA/DNA complex, because the local concentration of PMA

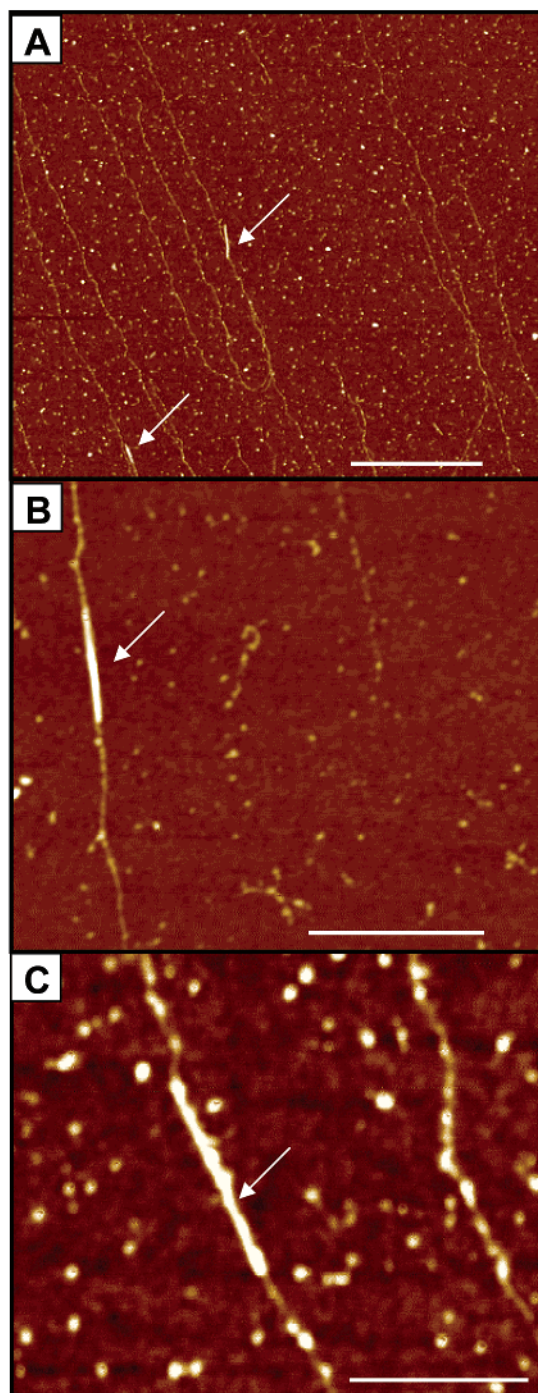


**Figure 2.** AFM height images of  $\lambda$ -DNA-templated SWNT positioning on Si surfaces. (A) Large area image of SWNTs deposited on PMA-treated DNA. White arrows indicate SWNTs; height scale is 12 nm, and the white bar indicates 1000 nm. (B, C) Smaller area images of two different substrates where SWNTs were deposited onto PMA-treated DNA. White arrows indicate SWNTs. The height scale is 18 nm and the white bar indicates 500 nm in (B), while the height scale is 4 nm and the white bar indicates 250 nm in (C).

is higher along the DNA than on the rest of the Si surface. For SWNTs with other orientations, the interaction usually is not strong enough to align SWNTs specifically on DNA. Finally, because DNA-templated SWNT assembly occurs only at the surface, the number of SWNTs available for binding to DNA is constrained by

the diffusion rate of SWNTs through the bulk solution. Utilizing recent advances in SWNT solubilization<sup>11,12</sup> should increase the number of SWNTs in solution and address the first limitation, while the use of active mixing during deposition should help to overcome the latter two constraints.

In conclusion, we have developed a technique to specifically localize SWNTs onto PMA-decorated  $\lambda$ -DNA molecules aligned on Si surfaces. With this method, over 60% of all SWNTs deposited on substrates are aligned on DNA fragments. We feel that this approach offers significant potential to facilitate the construction of ordered arrays of nanometer dimension materials. Finally, combining DNA-templated nanotube localization with the ability to form specific base pairs between oligonucleotide coupled nanostructures and surface DNA may enable the bottom-up construction of nanoscale electronic circuits.

**Acknowledgment.** We acknowledge partial support of this work from Brigham Young University and the donors of the Petroleum Research Fund, administered by the American Chemical Society. This work is also based upon work supported in part by The Army Research Laboratory and the U.S. Army Research Office under grant number DAAD19-02-1-0353.

## References

- (1) (a) Collins, P. G.; Zettl, A.; Bando, H.; Thess, A.; Smalley, R. E. *Science* **1997**, *278*, 100–103. (b) Tans, S. J.; Devoret, M. H.; Dai, H. J.; Thess, A.; Smalley, R. E.; Geerligs, L. J.; Dekker, C. *Nature* **1997**, *386*, 474–477. (c) Shim, M.; Javey, A.; Kam, N. W. S.; Dai, H. J. *J. Am. Chem. Soc.* **2001**, *123*, 11512–11513.
- (2) (a) Kong, J.; Franklin, N. R.; Zhou, C. W.; Chapline, M. G.; Peng, S.; Cho, K. J.; Dai, H. J. *Science* **2000**, *287*, 622–625. (b) Varghese, O. K.; Kichambre, P. D.; Gong, D.; Ong, K. G.; Dickey, E. C.; Grimes, C. A. *Sens. Actuators B* **2001**, *81*, 32–41. (c) Chopra, S.; Pham, A.; Gaillard, J.; Parker, A.; Rao, A. M. *Appl. Phys. Lett.* **2002**, *80*, 4632–4634. (d) Pengfei, Q. F.; Vermesh, O.; Grecu, M.; Javey, A.; Wang, O.; Dai, H. J.; Peng, S.; Cho, K. J. *Nano Lett.* **2003**, *3*, 347–351. (e) Valentini, L.; Armentano, I.; Kenny, J. M.; Cantalini, C.; Lozzi, L.; Santucci, S. *Appl. Phys. Lett.* **2003**, *82*, 961–963.
- (3) (a) Messer, B.; Song, J. H.; Yager, P. D. *J. Am. Chem. Soc.* **2000**, *122*, 10232–10233. (b) Cui, Y.; Lieber, C. M. *Science* **2001**, *291*, 851–853.
- (4) (a) Joselevich, E.; Lieber, C. M. *Nano Lett.* **2002**, *2*, 1137–1141. (b) Nagahara, L. A.; Amlani, I.; Lewenstein, J.; Tsui, R. K. *Appl. Phys. Lett.* **2002**, *80*, 3826–3828.
- (5) (a) Melosh, N. A.; Boukai, A.; Diana, F.; Gerardot, B.; Badolato, A.; Petroff, P. M.; Heath, J. R. *Science* **2003**, *300*, 112–115. (b) Artemyev, M.; Möller, B.; Woggon, U. *Nano Lett.* **2003**, *3*, 509–512.
- (6) (a) Braun, E.; Eichen, Y.; Sivan, U.; Ben-Yoseph, G. *Nature* **1998**, *391*, 775–778. (b) Richter, J.; Mertig, M.; Pompe, W.; Mönch, I.; Schackert, H. K. *Appl. Phys. Lett.* **2001**, *78*, 536–538. (c) Ford, W. E.; Harnack, O.; Yasuda, A.; Wessels, J. M. *Adv. Mater.* **2001**, *13*, 1793–1797. (d) Patolsky, F.; Weizmann, Y.; Lioubashevski, O.; Willner, I. *Angew. Chem., Int. Ed.* **2002**, *41*, 2323–2327. (e) Keren, K.; Kreuger, M.; Gilad, R.; Ben-Yoseph, G.; Sivan, U.; Braun, E. *Science* **2002**, *297*, 72–75. (f) Monson, C. F.; Woolley, A. T. *Nano Lett.* **2003**, *3*, 359–363.
- (7) Woolley, A. T.; Kelly, R. T. *Nano Lett.* **2001**, *1*, 345–348.
- (8) The SWNT suspension was prepared by sonicating 0.4 mg of SWNTs in 4 mL of DMF for 20 h in an ultrasonic bath.
- (9) Images were obtained with a Multimode IIIa AFM instrument with microfabricated Si cantilever tips (Veeco, Sunnyvale, CA). Vibrational noise was minimized using an active isolation system (MOD1-M, Halcyonics, Goettingen, Germany). Typical imaging parameters were (a) tip resonance frequency, 55–65 kHz; (b) free oscillation amplitude, 0.9–1.1 V; (c) setpoint, 0.4–0.7 V; (d) scan rate, 1.2–1.6 Hz. Images were processed offline to remove the background slope using software bundled with the AFM instrument.
- (10) The average height of the PMA features on the DNA exceeds that of the underlying DNA by 1.5 nm, while the nonspecifically deposited PMA features extend 2.6 nm (on average) above the surface. Since the molecular dimension of PMA on its longest axis is <1.0 nm, the heights of the elevated round features in Figure 1 are consistent with PMA clusters rather than individual molecules.
- (11) Chen, R. J.; Zhang, Y.; Wang, D.; Dai, H. *J. Am. Chem. Soc.* **2001**, *123*, 3838–3839.
- (12) Star, A.; Steuerman, D. W.; Heath, J. R.; Stoddart, J. F. *Angew. Chem., Int. Ed.* **2002**, *41*, 2508–2512.

JA035902P